IET Communications

Research Article

IET Journals
The Institution of Engineering and Technology

Channel model proposal for indoor relay-assisted power line communications

ISSN 1751-8628
Received on 18th August 2017
Revised 10th February 2018
Accepted on 1st March 2018
E-First on 21st May 2018
doi: 10.1049/iet-com.2017.0782
www.ietdl.org

Xiaolin Wu[1], Bin Zhu[2] ✉, Yue Rong[3]

[1]*School of Communication and Information Engineering, Chongqing University of Posts and Telecommunications, Chongqing, People's Republic of China*

[2]*College of Communication Engineering, Chongqing University, Chongqing, People's Republic of China*

[3]*Department of Electrical and Computer Engineering, Curtin University, Western Australia, Australia*

✉ *E-mail: zhubin@cqu.edu.cn*

Abstract: Due to its tree-like topology, the point-to-point (P2P) indoor power line communication (PLC) channel exhibits a similar broadcasting property as the wireless propagation channel shows. However, after relay nodes are introduced, the relay-assisted PLC (RaPLC) channel shows some notable differences compared with its wireless counterpart. A lot of results about the relay-assisted wireless channel can be found in the literature, but the work of modelling RaPLC channel has rarely been discussed in detail. As the first attempt to fill this gap, we apply the ABCD method to compute the channel transfer function (CTF) of the RaPLC channel. It has been clarified that, in general, the CTF of RaPLC channel cannot be obtained as a cascade of two independent P2P PLC sub-channels located on two sides of the relay node. Also, it is shown that the challenge of generating CTF of the RaPLC channel can be transformed into a group of equivalent P2P PLC channel modelling tasks. Under the time-division duplexing constraint, the relay node changes its working mode from the receiving phase to the transmitting phase, which shows that the RaPLC channel is abruptly time-varying in nature. Following the hybrid bottom-up approach, a statistical channel model with a simple six-segment indoor power grid topology has been developed for simulation. Practical measurements and numerical examples verify our results.

1 Introduction

The idea of using power lines for communication purposes has been existing for a long time. The most obvious advantage of power line communication (PLC) technology is the world-wide availability of electrical infrastructures [1]. Theoretically, it provides the natural solution to the Smart Grid construction by upgrading the existing traditional power grids.

To design reliable and advanced PLC systems, the knowledge of PLC channel characteristics is required. A great number of efforts have been made to the power line channel modelling topic. Depending on their modelling approaches, the models in the literature can be classified into two groups, namely, the top-down approach [2–5] and the bottom-up approach [6–10].

The top-down approach characterises the external behaviour characteristics of the PLC networks and uses a set of high-level parameters to describe the channel either in the time domain, e.g. [11], or in the frequency domain, e.g. [12]. The parameter values are usually derived from the statistical analysis based on the extensive measurement campaigns. The advantage of this approach is its low complexity. Once the model and parameters are given, numbers of channel realisations can be generated within a short period of time. However, despite the difficulty of setting a large number of test loops with the selection of physical characteristics and configurations, the results of this top-down approach lack connections with the physical topology. The bottom-up approach starts from a physical model and derives a group of low-level parameters to represent a particular indoor PLC channel. This approach ensures a strong connection with physical structures. Usually, the signal propagation characteristics can be tackled in the frequency domain. However, for indoor PLC channels, it is a hard task to define a fixed structural model which can represent the various physical network behaviours. As a trade-off, the authors of [13] proposed a hybrid model. This model provides physics-oriented channel simulations by setting values to a simplified network structure. In addition, statistical distributions for the low-level parameters of this structure are suggested so that generation of random channels is also allowed.

Note that despite their different modelling approach and parametrising methods, almost all current PLC models concentrate on the point-to-point (P2P) channel case.

Recently, the emerging cooperative communication technology has been adopted in the indoor PLC environment, e.g. [14, 15]. Fig. 1 shows a general three-node/two-phase relay system, where the relay node works in the time-division duplexing (TDD) mode. Under this configuration, the source node broadcasts a signal to the relay and destination nodes in the first phase, and in the second phase, the source node repeats a transmission of the same message to the destination node, while the relay node forwards its received signal to the destination node after certain signal processing. We refer to this as the broadcast-and-multi-access (BMA) relay scheme, which includes several special cases. If the source node remains silent in the second phase, the system becomes a broadcast-and-forward (BF) relay scheme. If the direct source-to-destination path is not available, then the system degenerates to a two-hop relay system.

In the above relay scheme, some special channel characteristics have been observed by the introduction of the extra relay node, which is beyond the description of the current P2P PLC channel models. We refer this case as the relay-assisted PLC (RaPLC) channel.

On the other hand, due to the tree-like topology of the power grid, the PLC network exhibits broadcasting characteristics among source nodes, relay nodes, and destination nodes. This is similar to the broadcasting characteristics of the wireless signal prorogation. However, some notable differences also exist between the RaPLC channel and its wireless counterpart. Firstly, in wireless scenarios, the source-to-destination, source-to-relay and relay-to-destination paths can be treated as independent of each other, and they usually share the same channel model; on the contrary, in the PLC environment the three signalling paths are highly correlated, as they share the same power cable grid and their change of impedance influence each other. Moreover, in a wireless

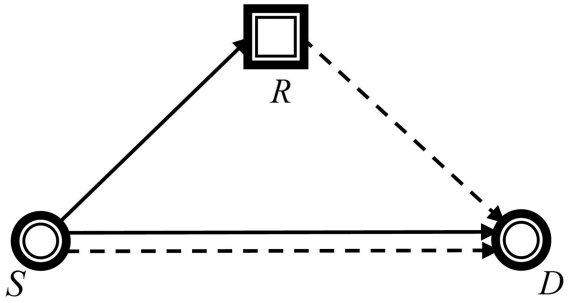

Fig. 1 *General three-node/two-phase relay scheme, where S, R and D stand for the source node, the relay node and the destination node, respectively. The first and second signalling phases are indicated by the solid-line and dash-line, respectively*

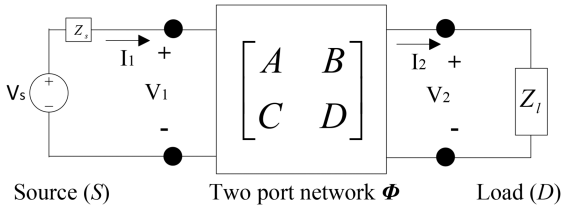

Fig. 2 *P2P PLC system represented by a two-port network* Φ

environment, the introduction of relay nodes does not influence the characteristics of the source-to-destination path given that the distance between the transceivers is much larger than the size of the relay device; however, in the PLC scenario, the appearance of the relay device will affect each path gain. In addition, for a wireless two-hop channel, the channel transfer function (CTF) can be usually obtained by cascading two independent sub-channels, which are located on the two sides of the wireless relay node; but as we will show in this work, it is not so straightforward for RaPLC channels.

The above differences were firstly mentioned in [16], but have rarely been studied in detail. Note that establishing realistic test platforms is a necessary precondition for evaluating different relay schemes used in the PLC environment. Thus, new channel models are required to characterise RaPLC channels. Following the hybrid bottom-up approach proposed in [13], in this work, we would like to investigate the RaPLC channel, where the relay nodes work in a frequency division duplexing manner, and propose a feasible simulation model for this channel.

The reminder of this work is organised as follows. In Section 2, we first briefly introduce the CTF computation of a P2P PLC channel by using the chain matrix theory from the transmission line theory. Next, in Section 3, we derive the CTF expressions of different signalling paths existing in the RaPLC channel and show that the challenge of generating the CTF of a RaPLC channel can be transferred into a group of equivalent P2P PLC channel modelling tasks. Following the hybrid bottom-up modelling approach in [13], in Section 4, a six-segment PLC topology has been used to simulate the RaPLC channel. Some typically numerical examples are given in Section 5 to verify our results. Lastly, Section 6 concludes this work.

2 CTF for P2P PLC channel

It is reported in [6] that every pair of outlets of the indoor power grid can be employed as a P2P communication system, and the corresponding channel is characterised by the wiring topology and load impedance between these two outlets. Let us refer to the outlet deployed transmitter as the source node S, and the other outlet deployed receiver as the destination node D. It is custom to refer to the shortest cabling link between the outlet pair as the backbone and its length as the P2P PLC channel's length [6]. Other cables are treated as branches attached to the backbone, which contribute to the multipath nature of the indoor P2P PLC channel. If we denote the CTF of the signalling path from L_1 to L_2 as $H_{L_1L_2}(f)$, where L_1 and L_2 are two network nodes, while f means the frequency [Unless necessary, we drop the notation of the frequency f in the following CFT expressions.]. Then, for P2P PLC channels, the symmetry property reported in [17] can be written as

$$\hat{H}_{SD} = \hat{H}_{\mathrm{DS}}. \tag{1}$$

2.1 ABCD matrix

The general representation of a P2P PLC network in the ABCD method is shown in Fig. 2, where the ideal voltage source V_s cascading its corresponding inner impedance Z_s is used to build the information source S, while the load impedance Z_L represents the receiver D. The PLC network Φ, in the middle, is represented by the two-port network ABCD model. In the two-port network, the input voltage V_1, input current I_1, output voltage V_2 and out current I_2, in general, hold the relations as

$$\begin{bmatrix} V_1 \\ I_1 \end{bmatrix} = \begin{bmatrix} A & B \\ C & D \end{bmatrix} \begin{bmatrix} V_2 \\ I_2 \end{bmatrix}, \tag{2}$$

where A, B, C, and D are appropriately chosen constants, which only depend on the inner topology and components of the two-port network and are not influenced by the outside associated circuits.

It is easy to show that if there is a direct cascade of two-port circuits, e.g. Φ_1 and Φ_2, the ABCD representation of this cascaded circuit, e.g. Φ_0, is the matrix multiplication of the ABCD matrices of the two individual two-port circuits, i.e.

$$\begin{aligned} \boldsymbol{\Phi}_0 &= \begin{bmatrix} A_0 & B_0 \\ C_0 & D_0 \end{bmatrix} \\ &= \begin{bmatrix} A_1 & B_1 \\ C_1 & D_1 \end{bmatrix} \begin{bmatrix} A_2 & B_2 \\ C_2 & D_2 \end{bmatrix} \\ &= \boldsymbol{\Phi}_1 \boldsymbol{\Phi}_2 . \end{aligned} \tag{3}$$

2.2 Transfer function from ABCD matrix

Using the ABCD model in Fig. 2, it is straightforward to calculate the transfer function between the voltage source and the receiving (Rx) load as

$$\begin{aligned} H_{\Phi} &= \frac{V_1}{V_s} \\ &= \frac{Z_l}{AZ_l + B + CZ_lZ_s + DZ_s}. \end{aligned} \tag{4}$$

From (4) we notice that the CTF of a network not only depends on its inner ABCD parameters but also depends on the inner impedance of its stimulating source (Z_s) and its connected load (Z_l).

3 CTF for RaPLC channel

In an indoor power grid, any outlet located on the backbone of the P2P channel or on a branch of this backbone can be deployed with a plug-in relay device. Obviously, in practice there is no way to understand whether the chosen outlet is connected to the backbone directly or to a branch. However, as the former outlet location can be treated as a special case of the latter one, without losing generality, we choose a branch-located outlet to deploy the relay device. We refer to this device as the relay node R as shown in Fig. 1.

After the introduction of the relay node into the P2P PLC channel, the power grid can be seen as consisting of three two-port networks and each of them can be represented by its ABCD matrix, i.e.

$$\boldsymbol{\Phi}_1 = \begin{bmatrix} A_1 & B_1 \\ C_1 & D_1 \end{bmatrix}, \tag{5}$$

$$\boldsymbol{\Phi}_2 = \begin{bmatrix} A_2 & B_2 \\ C_2 & D_2 \end{bmatrix}, \tag{6}$$

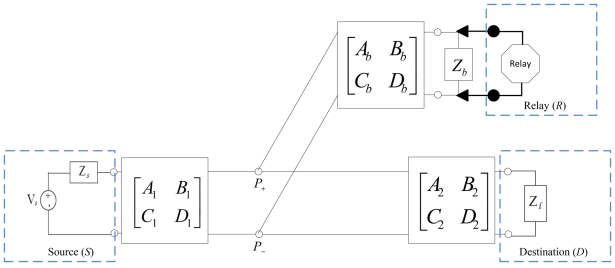

Fig. 3 *Circuit model for a general RaPLC channel*

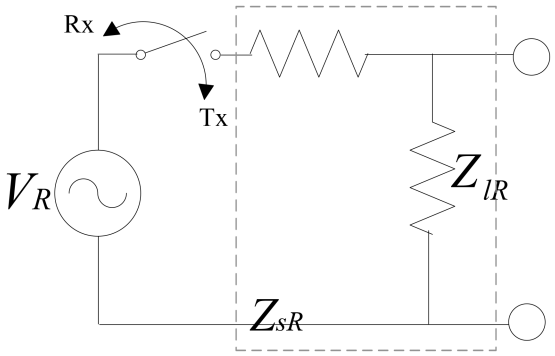

Fig. 4 *Two-state circuit model of the relay node*

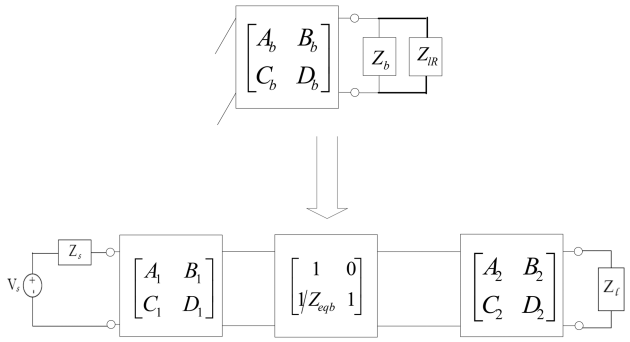

Fig. 5 *Equivalent P2P model for relay-assisted path gain* $H_{SD}^{(1)}$

$$\mathbf{\Phi}_{\mathrm{b}} = \begin{bmatrix} A_{\mathrm{b}} & B_{\mathrm{b}} \\ C_{\mathrm{b}} & D_{\mathrm{b}} \end{bmatrix}. \tag{7}$$

This has been shown in Fig. 3, where Z_{b} is a pre-existing load. Treat $Z_{\mathrm{b}} = \infty$, if there is no load pre-existing on the relay branch. The point P indicates the intersection of the relay located branch and the backbone. As TDD half-duplexing constrains hold (as shown in Fig. 1), relay schemes work in two signalling phases, which shows that up to four signalling paths exist under the RaPLC channel condition. If we denote the signalling path existing in the j th phase, from nodes L_1 to L_2, with its complex path gain $H_{L_1L_2}^{(j)}$, where $L_1 \in \{S, R\}$, $L_2 \in \{R, D\}$ and $j = 1, 2$. It is our task to derive the expressions of $H_{SD}^{(1)}$, $H_{SR}^{(1)}$, $H_{RD}^{(2)}$ and $H_{SD}^{(2)}$.

3.1 Modelling of the relay node

The relay node changes its working role in two different phases. Specifically, in the first phase the relay node works in the Rx mode and a load impedance Z_{lR} is appropriate to model it. While in the second stage, the relay node acts as a transmitting (Tx) source, which can be modelled by a controlled voltage source V_R and an inner impedance Z_{sR} as shown in Fig. 4. Usually, the value of Z_{lR} and Z_{sR} takes constant resistance, such as 5, 50 and 150 Ω.

3.2 Path gain $H_{SD}^{(1)}$

By using equivalent impedance technique discussed in Section 2, we can convert the relay branch into its equivalent two-port network at intersection point P. This has been illustrated in Fig. 5, where the input equivalent impedance of the relay branch Z_{eqb} is computed as

$$Z_{\mathrm{eqb}} = \frac{A_{\mathrm{b}} Z_{\mathrm{lR}}' + B_{\mathrm{b}}}{C_{\mathrm{b}} Z_{\mathrm{lR}}' + D_{\mathrm{b}}}, \tag{8}$$

where Z_{lR}' is the paralleling equivalent impedance of Z_{b} and Z_{lR}, namely

$$\begin{aligned} Z_{\mathrm{lR}}' &= Z_{\mathrm{b}} // Z_{\mathrm{lR}} \\ &= \frac{Z_{\mathrm{b}} Z_{\mathrm{lR}}}{Z_{\mathrm{b}} + Z_{\mathrm{lR}}}. \end{aligned} \tag{9}$$

Thus the multiplication ABCD matrix from S to D in the first phase can be expressed as

$$\begin{aligned} \mathbf{\Phi}_{\mathbf{SD}}^{(1)} &= \begin{bmatrix} A_{SD}^{(1)} & B_{SD}^{(1)} \\ C_{SD}^{(1)} & D_{SD}^{(1)} \end{bmatrix} \\ &= \begin{bmatrix} A_1 & B_1 \\ C_1 & D_1 \end{bmatrix} \begin{bmatrix} 1 & 0 \\ \dfrac{1}{Z_{\mathrm{eqb}}} & 1 \end{bmatrix} \begin{bmatrix} A_2 & B_2 \\ C_2 & D_2 \end{bmatrix}. \end{aligned} \tag{10}$$

Using (4) with (10), it leads to the path gain $H_{SD}^{(1)}$ as

$$\begin{aligned} H_{SD}^{(1)} &= \frac{V_{\mathrm{l}}}{V_{\mathrm{s}}} \\ &= \frac{Z_{\mathrm{l}}}{A_{SD}^{(1)} Z_{\mathrm{l}} + B_{SD}^{(1)} + C_{SD}^{(1)} Z_{\mathrm{l}} Z_{\mathrm{s}} + D_{SD}^{(1)} Z_{\mathrm{s}}}. \end{aligned} \tag{11}$$

Note for the two-hop relay scheme case, we should treat $Z_{\mathrm{l}} \to 0$ in (11), as there is no direct path available.

3.3 Path gain $H_{SR}^{(1)}$

As in the first phase, the source node also broadcasts a signal to the relay node through the path from Φ_1 to Φ_{b} as shown in Fig. 6, from the relay node's point of view, the second segment Φ_2 on the backbone should be treated as a 'branch', where the input equivalent impedance of the Φ_2 branch is computed as

$$Z_{\mathrm{eq2}} = \frac{A_2 Z_{\mathrm{l}} + B_2}{C_2 Z_{\mathrm{l}} + D_2}. \tag{12}$$

Note when the two-hop relay scheme case is considered, we should treat $Z_{\mathrm{l}} \to 0$ in (12) as a direct link is not available. Thus the multiplication matrix from S to R in the first phase can be expressed as

$$\begin{aligned} \mathbf{\Phi}_{SR}^{(1)} &= \begin{bmatrix} A_{SR}^{(1)} & B_{SR}^{(1)} \\ C_{SR}^{(1)} & D_{SR}^{(1)} \end{bmatrix} \\ &= \begin{bmatrix} A_1 & B_1 \\ C_1 & D_1 \end{bmatrix} \begin{bmatrix} 1 & 0 \\ \dfrac{1}{Z_{eq2}} & 1 \end{bmatrix} \begin{bmatrix} A_{\mathrm{b}} & B_{\mathrm{b}} \\ C_{\mathrm{b}} & D_{\mathrm{b}} \end{bmatrix}, \end{aligned} \tag{13}$$

which in turn leads to the path gain $H_{SR}^{(1)}$ as

$$\begin{aligned} H_{SR}^{(1)} &= \frac{V_{\mathrm{lR}}}{V_{\mathrm{s}}} \\ &= \frac{Z_{\mathrm{lR}}'}{A_{SR}^{(1)} Z_{\mathrm{lR}}' + B_{SR}^{(1)} + C_{SR}^{(1)} Z_{\mathrm{lR}}' Z_{\mathrm{s}} + D_{SR}^{(1)} Z_{\mathrm{s}}}, \end{aligned} \tag{14}$$

where Z_{lR}' is the paralleling equivalent impedance of Z_{b} and Z_{lR}, i.e.

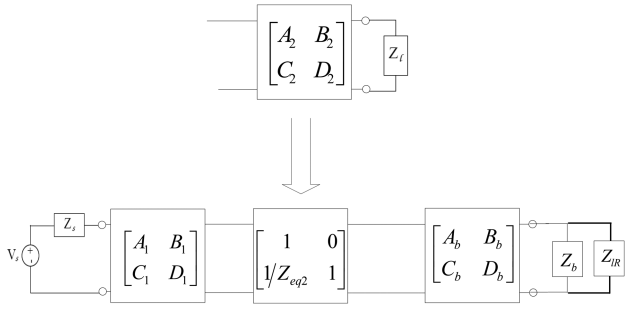

Fig. 6 *Equivalent P2P model for relay-assisted path gain* $H_{SR}^{(1)}$

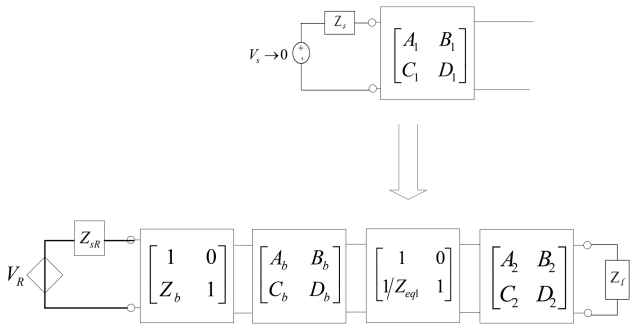

Fig. 7 *Equivalent P2P model for relay-assisted path gain* $H_{RD}^{(2)}$

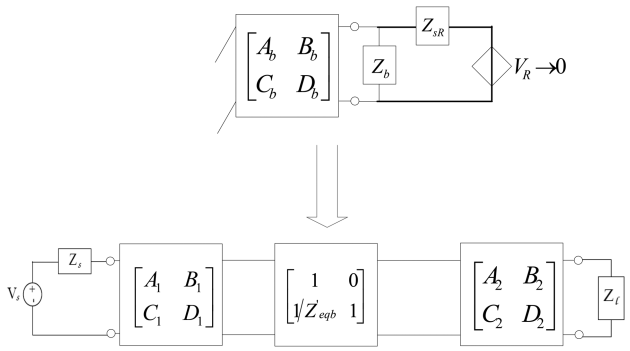

Fig. 8 *Equivalent P2P model for relay-assisted path gain* $H_{SD}^{(2)}$

$$Z_{\mathrm{lR}}^{'} = Z_{\mathrm{b}} // Z_{\mathrm{lR}} = \frac{Z_{\mathrm{b}} Z_{\mathrm{lR}}}{Z_{\mathrm{b}} + Z_{\mathrm{lR}}}. \tag{15}$$

3.4 Path gain $H_{RD}^{(2)}$

As in the second phase, the relay node works as a transmitter which forwards the signal to the destination node through the path from Φ_{b} to Φ_2 as shown in Fig. 7. From the destination node's point of view, the first segment Φ_1 on the backbone should be treated as a 'branch', where input equivalent impedance of the Φ_1 branch is computed as

$$Z_{\mathrm{eq1}} = \frac{A_1 Z_{\mathrm{s}} + B_1}{C_1 Z_{\mathrm{s}} + D_1}. \tag{16}$$

Note for the two-hop and BF relay schemes, the source should be treated as an open circuit (high impedance state) as it does not work in the second phase. This can be configured by setting $Z_{\mathrm{s}} \to \infty$ in (16); on the other hand, for the BMA relay scheme, the source node repeats a transmission. Following the superposition theorem, its transmission voltage V_{s} should be set as zero, as here we only intend to find the response on Z_{l} stimulated by the relay node's effect. With the ABCD expression of Z_{b}, the multiplication matrix from R to D in the second phase can be expressed as

$$\begin{aligned} \boldsymbol{\Phi}_{\mathbf{RD}}^{(2)} &= \begin{bmatrix} A_{RD}^{(2)} & B_{RD}^{(2)} \\ C_{RD}^{(2)} & D_{RD}^{(2)} \end{bmatrix} \\ &= \begin{bmatrix} 1 & 0 \\ Z_{\mathrm{b}} & 1 \end{bmatrix} \begin{bmatrix} A_{\mathrm{b}} & B_{\mathrm{b}} \\ C_{\mathrm{b}} & D_{\mathrm{b}} \end{bmatrix} \begin{bmatrix} 1 & 0 \\ \frac{1}{Z_{\mathrm{eq1}}} & 1 \end{bmatrix} \begin{bmatrix} A_2 & B_2 \\ C_2 & D_2 \end{bmatrix}. \end{aligned} \tag{17}$$

Again, by using (4), the path gain $H_{SR}^{(1)}$ can be calculated as

$$\begin{aligned} H_{RD}^{(2)} &= \frac{V_{\mathrm{l}}}{V_R} \\ &= \frac{Z_{\mathrm{l}}}{A_{RD}^{(2)} Z_{\mathrm{l}} + B_{SD}^{(2)} + C_{SD}^{(2)} Z_{\mathrm{l}} Z_{\mathrm{sR}} + D_{SD}^{(2)} Z_{\mathrm{sR}}}, \end{aligned} \tag{18}$$

where Z_{sR} is the inner impedance of the relay node when it works in the transmission mode.

3.5 Path gain $H_{SD}^{(2)}$

For the two-hop and BF relay schemes, there is no need to discuss this problem; on the other hand, in the BMA scheme, the source node repeats a transmission in the second phase. Again, as here we only have interest about the response on Z_{l} stimulated by the source node's effect, the relay node's transmission voltage V_R should be set as $V_R \to 0$, as shown in Fig. 8, where the input equivalent impedance of the relay branch Φ_{b} is computed as

$$Z_{\mathrm{eqb}}^{'} = \frac{A_{\mathrm{b}} Z_{\mathrm{lR}}^{''} + B_{\mathrm{b}}}{C_{\mathrm{b}} Z_{\mathrm{lR}}^{''} + D_{\mathrm{b}}}, \tag{19}$$

where $Z_{\mathrm{lR}}^{''}$ is the parallel equivalent impedance of Z_{b} and relay node's inner impedance Z_{sR}, namely

$$\begin{aligned} Z_{\mathrm{lR}}^{''} &= Z_{\mathrm{b}} // Z_{\mathrm{sR}} \\ &= \frac{Z_{\mathrm{b}} Z_{\mathrm{sR}}}{Z_{\mathrm{b}} + Z_{\mathrm{sR}}}. \end{aligned} \tag{20}$$

Thus the multiplication matrix from S to D in the second phase can be written as

$$\begin{aligned} \boldsymbol{\Phi}_{\mathbf{SD}}^{(2)} &= \begin{bmatrix} A_{SD}^{(2)} & B_{SD}^{(2)} \\ C_{SD}^{(2)} & D_{SD}^{(2)} \end{bmatrix} \\ &= \begin{bmatrix} A_1 & B_1 \\ C_1 & D_1 \end{bmatrix} \begin{bmatrix} 1 & 0 \\ \frac{1}{Z_{eqb}^{'}} & 1 \end{bmatrix} \begin{bmatrix} A_2 & B_2 \\ C_2 & D_2 \end{bmatrix}, \end{aligned} \tag{21}$$

which in turn leads to the path gain that

$$\begin{aligned} H_{SD}^{(2)} &= \frac{V_{\mathrm{l}}}{V_{\mathrm{s}}} \\ &= \frac{Z_{\mathrm{l}}}{A_{SD}^{(2)} Z_{\mathrm{l}} + B_{SD}^{(2)} + C_{SD}^{(2)} Z_{\mathrm{l}} Z_{\mathrm{s}} + D_{SD}^{(2)} Z_{\mathrm{s}}}. \end{aligned} \tag{22}$$

Above analysis has shown that the task of modelling a RaPLC channel can be transformed as generating a group of equivalent P2P PLC channels, while the latter ones can be calculated by using the ABCD method given the topology and load impedance information of a target PLC network. Furthermore, extending above analysis to the situations, where more than one relay node has been introduced, is straight forward.

It is worth to mention some findings. As the relay node changes its working mode from the first phase to the second phase and in general $Z_{\mathrm{sR}} \neq Z_{\mathrm{lR}}$, thus

$$H_{SD}^{(1)} \neq H_{SD}^{(2)}, \tag{23}$$

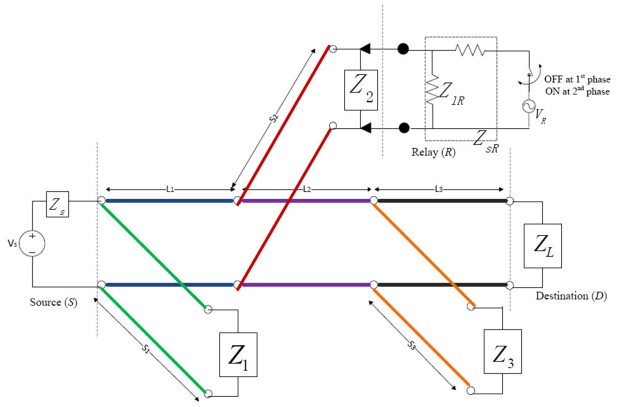

Fig. 9 *Topology of the six-segment relay-assisted channel model*

Table 1 Characteristic data of five common indoor power cables [13]

Cable type	1	2	3	4	5
ϕ, mm^2	1.5	2.5	4	6	10
ϵ_{eq}	1.45	1.52	1.56	1.73	2
Z_0 (Ω)	270	234	209	178	143
C, pF/m	15	17.5	20	25	33
L, μH/m	1.08	0.96	0.87	0.78	0.68
R_0	12	9.34	7.55	6.25	4.98
G_0	30.9	34.7	38.4	42.5	49.3

which indicates that the RaPLC channel is time-varying in nature, even each P2P path in the different phase can be assumed as time-invariant. Interestingly, if we compare the resulted path gains (11), (14), (18) and (22), we can also find that in general

$$H_{SD}^{(1)} \neq H_{SR}^{(1)} H_{RD}^{(2)}, \tag{24}$$

$$H_{SD}^{(2)} \neq H_{SR}^{(1)} H_{RD}^{(2)}. \tag{25}$$

In addition, the appearance of the impedance of the relay node changes the original P2P channel's topology and loading status. As a result, in general, the signalling path gain between the transceiver pair has varied, i.e.

$$\hat{H}_{SD} \neq H_{SD}^{(j)} \quad (j = 1, 2). \tag{26}$$

Combining (23) to (26), it is clarified that in general the CTF of RaPLC channel RaPLC can be obtained as a product of the CTFs of several independent P2P channels. Note these special characteristics distinguish RaPLC channels to their wireless counterparts.

4 Hybrid channel model proposal

4.1 Hybrid modelling methodology

In Section 3, it is shown that given the gird topology and load impedance information of a target PLC network, we can model its CTF by following the ABCD method. Moreover, if we adopt the indoor PLC random topology generator proposed in [6], an ensemble of statistical RaPLC channels can also be built. However, the computation of this 'ground-up' approach can be very intensive.

For its simple parametrisation system and measurement-verified performance, in this work, we follow the 'hybrid' approach proposed in [13], where a P2P PLC channel model has been built from a simplified network topology with statistical parameters chosen for the cables and loads. [This hybrid P2P model is publicly accessible. Its software and user's guide can be found in [18, 19].] Note its fixed topology simplifies the ABCD calculation of the network, while its random chosen cables and load parameters introduce the statistical property to this bottom-up model, so the 'hybrid' strategy is named.

4.2 Six-segment RaPLC channel model

A general RaPLC channel model has been given in Fig. 3. To simplify its topology realisation, one cable-pair segment with one terminated branch is used to represent each two-port network Φ_i ($i = 1, b, 2$) existing in Fig. 3. Thus, the topology of the proposed model is shown in Fig. 9. We can see that totally six segments are present in this model. Particularly, there are three segments on the backbone (i.e. $L_i, i = 1, 2, 3.$) between the transceivers (S and D) and three branch-taps (i.e. $S_i, i = 1, 2, 3.$), terminated with loading impedance Z_1, Z_2 and Z_3, respectively. The relay device (R) has been plugged in the second branch segment and paralleled with its pre-existing load Z_2. Note this topology has been chosen for its simple structure while, at the same time, not losing reasonable fit to the real channel behaviours.

As the modelling of relay device has been discussed in Section 3, we explain other parts of this model as follows.

4.2.1 Cables.: Each segment includes a power cable pair. In addition to its length L_i or S_i ($i = 1, 2, 3$), each cable pair is chartered by its type n_{L_i} or n_{S_i} ($i = 1, 2, 3$), which in turn depends on its manufacture parameters, namely the per-unit-length resistance R, inductance L, conductance G, capacitance C, characteristic impedance Z_0, and its equivalent dielectric constant ϵ_{eq} and section size ϕ. Five most commonly used cables with their characteristic data are given in Table 1, where $R = R_0 \cdot 10^{-5}\sqrt{f}$ (Ω/m), $G = G_0 \cdot 5 \cdot 10^{-14} \cdot 2\pi f$ (S/m), and f means the frequency.

4.2.2 Loads.: Based on the measurement of different electrical appliances' impedance behaviour, the authors of [20] report that the loading impedance, in an indoor power grid, can behave in three possible states, namely: (i) constant impedance; (ii) frequency-selective impedance; and (iii) linear periodical time-varying (LPTV) impedance. Note in the third case, the time-varying loading impedance makes the PLC network behave as an LPTV system. However, comparing its relative long coherent time, i.e. about 600 μs [20], to the period of a signalling phase in practical RaPLC systems, at most of the time, we can reasonably treat the PLC network as a linear quasi-time-invariable system in one signalling phase. This means the channel condition does not change given the network topology and loads remain constant in the current signalling phase. Note this does not indicate that the RaPLC channel, where more than one signalling phase and rapid changing loading impedance need to be considered, is also quasi-time-invariant, as we have shown in Section 3.

• When the load takes the constant impedance, it is recommended that using the value in the set of $\{5, 50, 150, 1000, \infty\}$ to represent different pure resistances and open circuit situation.
• For the frequency-selective impedance case, the frequency response of an RLC resonant circuit, i.e.

$$Z(f) = \frac{R}{1 + \mathrm{j}Q\left(\frac{2\pi f}{2\pi f_0} - \frac{2\pi f_0}{2\pi f}\right)} \tag{27}$$

is adequate to model it. In (27), R, f_0 and Q are the resonance resistance, resonance frequency, and quality factor, of the RLC resonant circuit, respectively.
• It is reported in [20] that two types of time-varying loading impedance appear in the indoor power grid, and both of them synchronise with the main voltage. For the harmonic behaviour type, we can model it with the expression

$$Z(f, t) = Z_A(f) + Z_B(f)\left|\sin(2\pi f_m t + \phi)\right|, \quad 0 < t < T_m, \tag{28}$$

where Z_A and Z_B can take the form of (27) or pure resistance values, while f_{m} and T_{m} are, respectively, the mains frequency and

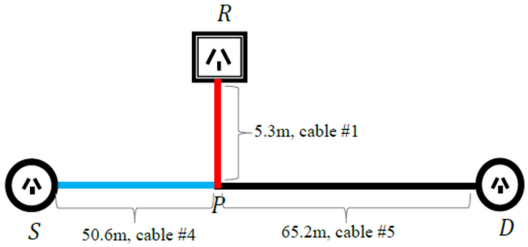

Fig. 10 *Topology of the simple three-segment testing channel*

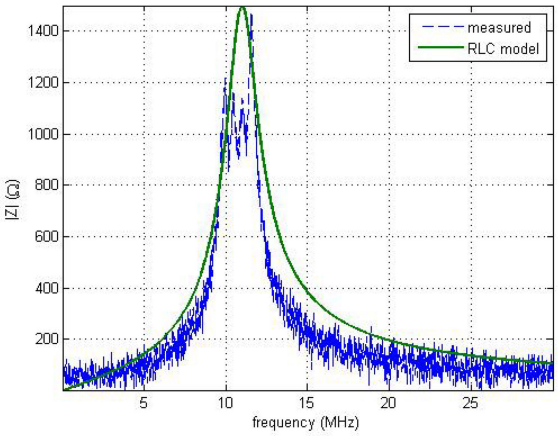

Fig. 11 *Frequency response of appliance impedance* Z_b

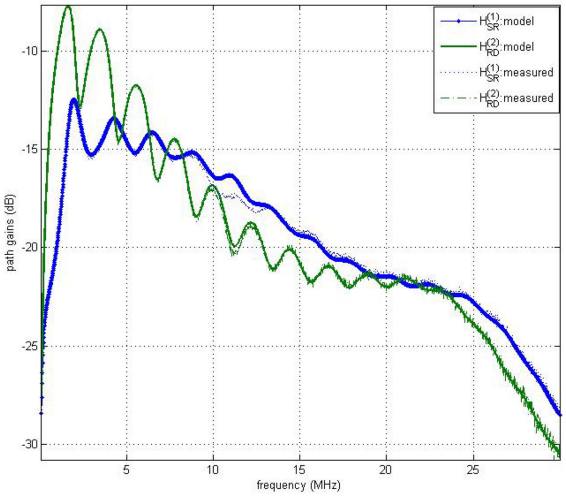

Fig. 12 *Amplitude responses of the source-to-relay and relay-to-destination paths of the testing channel*

mains period. [In China and Australia, the mains frequency and period are 50 Hz and 20 ms, respectively.] Here ϕ indicates an initial leading phase compared with the mains period. For the commuted behaviours situation, the expression

$$Z(f,t) = Z_A(f) + Z_B(f)|\text{rect}(2\pi f_m t, \gamma, D)|, \quad 0 < t < T_m \qquad (29)$$

is used to model it. In (29), rect(t) is similar to sin(t), but creates a square waveform with peaks of ± 1. Here D and γ indicate the initial delay (w.r.t mains period) and the duty of the positive peak in one cycle, respectively, while Z_A and Z_B hold the same property as in the harmonic case.

Using the ABCD method with a set of specific parameters discussed above, four different path gains (i.e. $H_{SD}^{(1)}$, $H_{SR}^{(1)}$, $H_{RD}^{(2)}$ and $H_{SD}^{(2)}$) existing in the six-segment RaPLC channel can be calculated.

4.3 Statistical parameters for random generation of sample channels

Based on the many channel testing and load measurements, along with some intuitive decision, the authors of [13] report a set of parameter values or ranges for their P2P model. Considering the RaPLC channel can be equivalently represented by a group of P2P paths, as we have shown in Section 3, we can readily adopt this measurement-verified parameter configuration in the above six-segment relay-assisted channel model. Those parameters with their statistical distributions are summarised in the Appendix.

5 Numerical examples

In this section, we present a series of RaPLC channel examples generated by the proposed six-segment model. On the one hand, we set up a simple testing channel, and use the real experiment measurement result as the benchmark to verify our model. On the other hand, for comparison purpose, we cite two classical P2P PLC channel models, namely the models in [2, 10], respectively, as benchmarks. Note that the reason of choosing these particular two models is because the model in [2] is the typical result of the 'top-down' modelling approach, while the model in [10] the 'bottom-up' approach.

5.1 Verification with experiment channel

To verify the validity of the proposed model, a simple three-segment testing topology as shown in Fig. 10 has been constructed and measured. Note different types of cables have been used for different segments of the network on purpose. The relay device is plugged into the only available branch, where a typical appliance (i.e. a desktop electric fan), with its loading impedance Z_b, has been deployed. The measured and modelled frequency response of the appliance impedance Z_b are given in Fig. 11, respectively. In Fig. 12, the amplitude responses of the source-to-relay and relay-to-destination paths from the measurement are compared with their corresponding results generated from the proposed model. It can be seen that the simulation and measured results match each other closely, which demonstrates that the proposed model can accurately predict the channel response of the RaPLC grid. Caused by the impedance of the branched loads, the attenuation notches can be observed in Fig. 12. Note about 1–3 dB difference appears at the notches around 11 MHz between the simulation and measured results. This is mainly due to the approximation between the actual impedance and the RLC modelled result of the branched appliance Z_b, as can be seen in Fig. 11.

5.2 Comparison with two P2P benchmark results

To examine the flexibility and versatility of the proposed model, let us remove the appliance Z_b from the testing topology (so now the relay branch is only loaded by the relay device) and get a group of path gains (i.e. $H_{SD}^{(1)}$, $H_{SD}^{(2)}$, $H_{SR}^{(1)}$ and $H_{RD}^{(2)}$) of the network as shown in Fig. 13. Also, for comparison purpose, we cite the models in [2, 10], respectively, and use the same testing setting as in Fig. 10 to obtain two corresponding P2P CTFs. We refer to these two benchmark CTFs as H_{P2P} [2] and H_{P2P} [10], respectively, in Fig. 13. Interestingly, we find that in the two benchmark P2P CTFs a heavy notch appears at around 12 MHz, but disappears in their corresponding path gains (i.e. $H_{SD}^{(1)}$ and $H_{SD}^{(2)}$) of the relay-assisted case. The reason behind this phenomenon is the appearance of the relay's impedance (i.e. Z_{lR} or Z_{sR}) changes the impedance mismatch between different segments of the network to some extent.

Besides, we can also find in Fig. 13 that the RaPLC path gains (i.e. $H_{SD}^{(1)}$, $H_{SD}^{(2)}$, $H_{SR}^{(1)}$ and $H_{RD}^{(2)}$) are correlated to each other at a certain degree. We will investigate this point deeper in the next subsection.

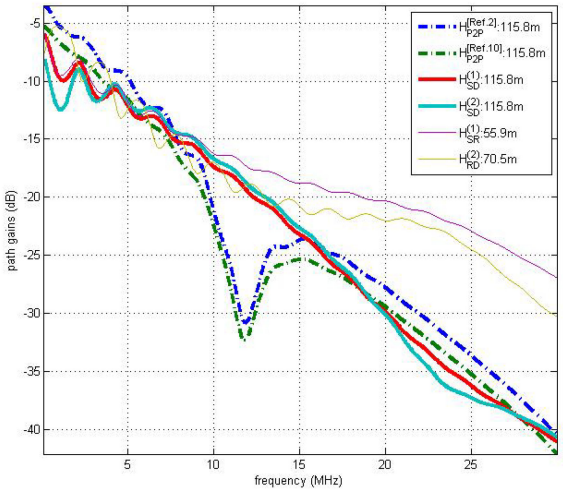

Fig. 13 *Group of path gains existing in the testing RaPLC network, where two benchmark P2P CTFs (H_{P2P} [2] and H_{P2P} [10]) have also been given for comparison*

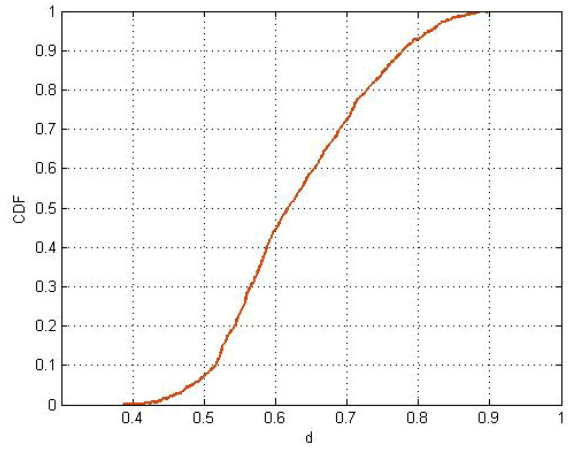

Fig. 14 *Empirical CDF for the ADC of 1000 random RaPLC channel realisations*

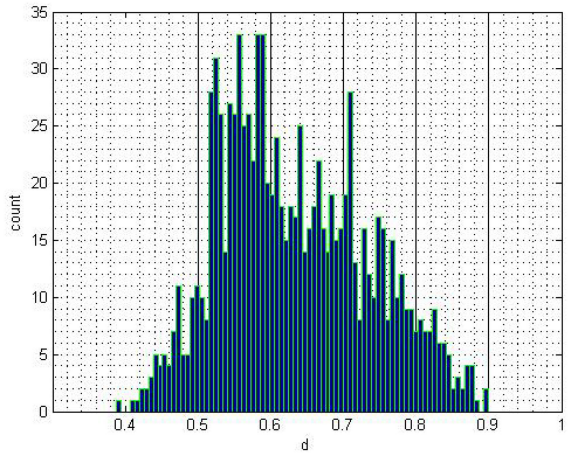

Fig. 15 *Empirical histogram for the ADC of 1000 random RaPLC channel realisations*

5.3 Correlation property of RaPLC channel

To further explore this correlation property of RaPLC channels in a general sense, let us first use X_i (i=1,2,3,4) to denote the magnitude of the grouped path gains $|H_{SD}^{(1)}|$, $|H_{SR}^{(1)}|$, $|H_{RD}^{(2)}|$ and $|H_{SD}^{(2)}|$, respectively. Then, the average degree of correlation (ADC) of each four-path group can be defined as

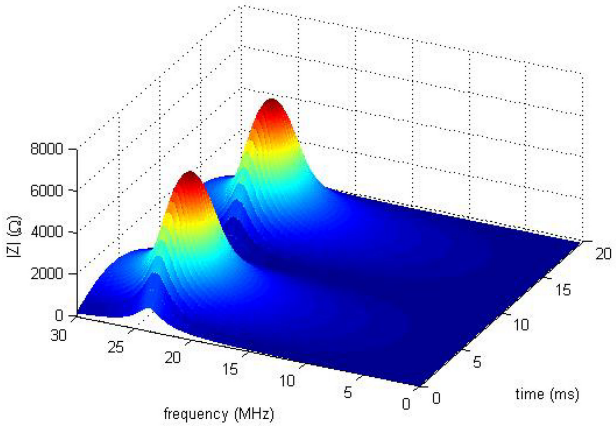

Fig. 16 *Time-varying frequency response of the harmonic impedance*

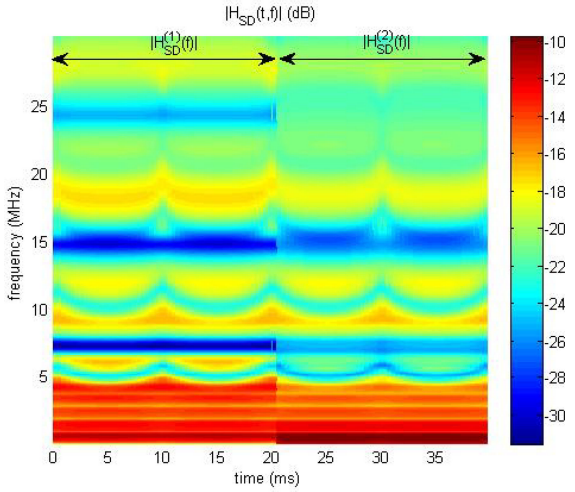

Fig. 17 *Rapid change of the source-to-destination path gain H_{SD} at the transient moment*

$$d = \sqrt{\frac{\sum_{i,j}(\rho_{i,j})^2}{N_\rho}}, \quad i > j \quad \text{and} \quad i, j = 1, 2, 3, 4, \tag{30}$$

where N_ρ denotes the total number of $\rho_{i,j}$ and

$$\rho_{i,j} = \frac{\mathrm{Cov}(X_i, X_j)}{\sqrt{D(X_i)}\sqrt{D(X_j)}}, \tag{31}$$

where $\mathrm{Cov}(\cdot)$ and $D(\cdot)$ represent the covariance and variance operations, respectively. From the definition (30), it is easy to see that the value of d fall into the interval $[0, 1]$. The greater value d takes, the more correlative the four signalling paths present.

A total of 1000 channel samples are randomly generated, and the value of ADC for each one of them has been calculated by using (30). Figs. 14 and 15 depict the empirical histogram and cumulative distribution function (CDF) for the ADC of these generated channels. The sample mean and variance of d are 0.6334 and 0.0109, respectively, which indicates that most of the channel (four-path group) samples exhibit a relatively high correlation degree. This result corresponds to our intuition as the different paths share the same indoor power grid.

5.4 Rapidly time-varying nature of RaPLC channel

As we discussed in Section 3 that the sudden change of the relay's working mode from the first phase to the second phase causes the rapidly time-varying nature of RaPLC channels. To demonstrate this property, a sample channel including a harmonic LPTV impedance (with its time-varying frequency response shown in Fig. 16) has been generated. For easier observation, the signalling period of each phase of the relay node has been set as the same as

the mains period, i.e. 20 ms, on purpose. Its source-to-destination path gain from the first phase ($H_{SD}^{(1)}$) to the second phase ($H_{SD}^{(2)}$) have been shown in Fig. 17. It can be seen that in each signalling phase, i.e. [0,20) ms and [20,40) ms, the frequency response of this LPTV channel varies periodically along with half of the main period (i.e. 10 ms) in a harmonic manner. However, at the transient moment (i.e. 20 ms), the rapid transition happens due to the work mode transferring action of the relay node.

These simulation results verify the conclusions that we have drawn in Section 3.

6 Conclusion

In contrast to the wireless relaying scenario, an RaPLC channel presents high correlation among different paths. Appearance of any branched circuit connection (including the relay device itself) affects the CTFs of each signalling path. Based on the transmission line theory and the equivalent impedance technique, we applied the general ABCD method to compute the CTF of the RaPLC channel. Our discussion shows that the relay-assisted channel CTF generation problem can be transformed equivalently into a group of P2P PLC model cases. Following the hybrid bottom-up approach, a six-segment PLC topology has been proposed to generate the four different path gains of a RaPLC channel. Deterministic and random generated channel samples have been used to verify the validity of this model. It is hoped that the model can be used to build realistic test platforms for evaluating the performance of various relay schemes under PLC scenarios.

7 Acknowledgments

The authors would like to thank Mr Shui Wen for his kind help with the experiment preparation and measurement results recording. Part of this work was supported by the Fundamental Research Funds for the Central Universities of China, with project no. 106112016CDJCR161204 and the National Natural Science Foundation of China (no. 61571069).

8 References

[1] Mudriievskyi, S.: 'Power line communications: state of the art in research, development and application', *AEU-Int. J. Electron. Commun.*, 2014, **68**, (7), pp. 575–577

[2] Zimmermann, M., Dostert, K.: 'A multipath model for the powerline channel', *IEEE Trans. Commun.*, 2002, **50**, (4), pp. 553–559

[3] Galli, S., Banwell, T.C.: 'Modeling the indoor power line channel: new results and modem design considerations'. 2004 First IEEE Consumer Communications and Networking Conf. (CCNC 2004), Las Vegas, USA, 2004, pp. 25–30

[4] Galli, S., Banwell, T.: 'A novel approach to the modeling of the indoor power line channel-part ii: transfer function and its properties', *IEEE Trans. Power Deliv.*, 2005, **20**, (3), pp. 1869–1878

[5] Philipps, H.: 'Modelling of powerline communication channels'. Conf. IEEE Int. Symp. on Power Line Communications and its Applications, Lancaster, UK, 1999, pp. 14–21

[6] Tonello, A.M., Versolatto, F.: 'Bottom-up statistical PLC channel modeling–Part I: Random topology model and efficient transfer function computation', *IEEE Trans. Power Deliv.*, 2011, **26**, (2), pp. 891–898

[7] Tonello, A.M., Zheng, T.: 'Bottom-up transfer function generator for broadband PLC statistical channel modeling'. 2009 IEEE Int. Symp. on Power Line Communications and its Applications (ISPLC 2009), Dresden, Germany, 2009, pp. 7–12

[8] Sartenaer, T., Delogne, P.: 'Powerline cables modelling for broadband communications'. Proc. IEEE Int. Conf. Power Line Communications and its Applications, Malmö, Sweden, 2001, pp. 331–337

[9] Esmailian, T., Kschischang, F., Gulak, P: 'An in-building power line channel simulator'. Int. Symp. on Power Line Communications and its Applications (ISPLC), Athens, Greece, 2002, pp. 27–29

[10] Esmailian, T., Kschischang, F.R., Gulak, P.G.: 'In-building power lines as high-speed communication channels: channel characterization and a test channel ensemble', *Int. J. Commun. Syst.*, 2003, **16**, (5), pp. 381–400

[11] Galli, S.: 'A novel approach to the statistical modeling of wireline channels', *IEEE Trans. Commun.*, 2011, **59**, (5), pp. 1332–1345

[12] Tlich, M., Zeddam, A., Moulin, F., *et al.*: 'Indoor power-line communications channel characterization up to 100 MHz part I: one-parameter deterministic model', *IEEE Trans. Power Deliv.*, 2008, **23**, (3), pp. 1392–1401

[13] Canete, F., Cortes, J., Diez, L., *et al.*: 'A channel model proposal for indoor power line communications', *IEEE Commun. Mag.*, 2011, **49**, (12), pp. 166–174

[14] Tonello, A.M., Versolatto, F., D'Alessandro, S.: 'Opportunistic relaying in in-home PLC networks'. 2010 IEEE Global Telecommunications Conference (GLOBECOM 2010), Miami, USA, 2010, pp. 1–5

[15] Tan, B., Thompson, J.: 'Relay transmission protocols for in-door powerline communications networks'. 2011 IEEE Int. Conf. Communications Workshops (ICC), Kyoto, Japan, 2011, pp. 1–5

[16] Lampe, L., Vinck, A.H.: 'A study on relay network techniques in PLC'. The Workshop on Power Line Communications (WSPLC 2011), Arnhem, Netherlands, 2011

[17] Banwell, T., Galli, S.: 'On the symmetry of the power line channel'. Proc. Int. Symp. Power-Lines Communications, Malmö, Sweden, 2001, pp. 325–330

[18] 'PLC channel generator v2'. Available at http://www.plc.uma.es, Working Group on Power Line Communications, Communications Engineering Department, University of Malaga, accessed 3 May 2015

[19] 'User guide v2'. Available at http://www.plc.uma.es, Working Group on Power Line Communications, Communications Engineering Department, University of Malaga, accessed: 3 May 2015

[20] Corripio, F.C., Arrabal, J.A.C., del Rio, L.D., *et al.*: 'Analysis of the cyclic short-term variation of indoor power line channels', *IEEE J. Sel. Areas Commun.*, 2006, **24**, (7), pp. 1327–1338

9 Appendix

This Appendix presents Table 2, which contains the statistical parameters of the proposed RaPLC model. Those parameters with their statistical distributions are used for random generation of sample channels, such as the ones shown in Section 5. Note in the following Table 2, the shorthand 'd.u.d.a' is used for 'discrete uniform distribution among'.

Table 2 Distribution of random parameters

Parameter name	Symbol	Distribution	Unit
cable length	$L_i, S_i (i = 1, 2, 3)$	$\sim U[0.5, 50]]$	m
cable type	$n_{L_i}, n_{S_i} (i = 1, 2, 3)$	d.u.d.a {1,2,…,5}	N/A
source (relay Tx) impedance	$Z_{\mathrm{s}}(Z_{\mathrm{sR}})$	d.u.d.a {5,50,150}	Ω
destination (relay Rx) impedance	$Z_{\mathrm{l}}(Z_{\mathrm{lR}})$	d.u.d.a {50,150,1000}	Ω
constant impedance	$Z_i (i = 1, 2, 3)$	d.u.d.a {5,50,150,1000, ∞ }	Ω
RLC resonator: resonant resistance	R	$\sim U[200, 1800]$	Ω
RLC resonator: resonant frequency	f_0	$\sim U[2, 28]$	MHz
RLC resonator: quality factor	Q	$\sim U[5, 25]$	N/A
harmonic impedance: initial leading phase	ϕ	$\sim U[0, \pi]$	rad
commuted impedance: duty of positive peak	γ	$\sim U(0, 1)$	N/A
commuted impedance: the initial delay	D	$\sim U[0, T_{\mathrm{m}}(1 - \gamma)/2]$	s